Iris Recognition System Based on Texture Features

Suhad A. Ali[1], Dr. Loay E. George[2]
[1] Babylon University /Computer Science, Babylon, Iraq
Email: suhad_ali2003@yahoo.com
[2] Baghdad University /Computer Science, Baghdad/ Iraq
Email: loayedwar57@yahoo.com

Abstract— **Nowadays iris recognition becomes one of the most common methods for identification like password, keys, etc. In this paper, a new iris recognition system based on texture has been proposed to recognize persons using low quality iris images. At first, the iris area is located, and then a new method for eyelash and eyelid detection is applied, the introduced method depends on making image statistical analysis, to isolate the unwanted eyelash/eyelid areas from the true iris area. For discrimination purpose a set of texture features determined from the Haar wavelet subbands is used. Here, the iris area is divided into overlapping blocks and the average energy of each Haar wavelet sub-band is determined to be used as a local feature indicator. Also, the new method depends on using a weighted overlap blocking algorithm to build the iris code. To evaluate the performance of proposed method, it was applied to identify a set of iris images taken from CASIA V4.0 (interval class) data set and CASIA V1 dataset. The test results indicated that the new method give good recognition rates (i.e., 100%) with small size of features vector for CASIA V4.0 and (99.2%) for CASIA V1 dataset.**

Index Terms— **biometric, iris recognition, Haar wavelet, texture feature, local enhancement.**

I. INTRODUCTION

Biometrics is the science of establishing the identity of an individual based on the physical, chemical or behavioural attributes of the person. The relevance of biometrics in modern society has been reinforced by the need for large-scale identity management systems whose functionality relies on the accurate de-termination of an individual's identity in the context of several different applications [1, 2]. Iris recognition is one of the most reliable and accurate biometrics that play an important role in identification of individuals. The history of using iris as an identity of individual goes back to mid-19th-century when the French physician, Alphonse Bertillon, studied the use of eye color as an identifier [3].

Several researchers in the field of human recognition have been conducted and investigated the iris recognition methods. Iris recognition system consist of four stages which are iris information acquisition (still image/video), iris segmentation, iris pattern analysis, and iris pattern matching for eventual recognition [4]. Most of conducted researches in field iris recognition system deal with one of problems that found in steps of iris recognition system in order to get accurate results. The existing iris recognition approaches roughly into four major categories based on feature extraction scheme, namely, the phase-based methods [5, 6,7], the zero-crossing representation methods [8], the texture analysis-based methods [9,10,11,12,13], and the intensity variation analysis [14,9] methods. The most well-known one is that proposed by Daugman [5] who become the inventor of the most successful commercial iris recognition system now. Boles [15] decomposed one-dimensional intensity signals computed on circles in the iris and use zero-crossing of the decomposed signals for the feature extraction. Lima et al.[16] adopted texture analysis approach, in this approach a multi-channel Gabor filtering to capture both global and local details in an iris image. Recently, several researchers interest with iris recognition field.   Sheeba and et al [17] proposed method in 2013 to build security system using iris, in their method the Local Binary Pattern (LBP) is used to extract texture features and Learning Vector Quantization (LVQ)

method is used for classification. Lenina et al. [18] suggested the use ridgelets transforms to extract textural data. The proposed method was tested only on 33 subjects from CASIA V.3 interval class. This method skips normalization step. The method achieved accuracy 99.82%, 0.1309%FAR, 0.0434%FRR. Kshamaraj et al [19] proposed iris recognition method in 2012 using Independent Component Analysis for feature extraction. The iris region was detected using Daugman's method. For matching stage Euclidian distance was used between the test image and training image. The method was testes on 10 persons from CASIA V.1. The accuracy rate was 89.5%.

In this paper, a novel and relatively efficient method for iris recognition which falls in the second category "the texture analysis-based methods". This method is based on iris feature extraction which uses wavelet features such as energy and standard deviation. This method could improve system recognition accuracy since it depends on dividing iris region into blocks and assign weight (i.e. importance degree) for each block.

II. PROPOSED SYSTEM

As presented in fig.1, the proposed iris recognition system passes through four stages: iris localization, iris enhancement, features extraction and pattern matching.

A. *Iris Localization*

This stage aims to allocate and extract the iris region from the input eye image; it consists of three main steps:

Step-1: (Iris detection)
The iris region is allocated using our introduced method described in [20]. In this method, a sophisticated iris localization method is developed using a set of image processes; such as intensity thresholding, image equalization, smoothing, and some morphological operations. Both image intensity thresholding and some morphological operations are used to allocate the pupil region. While, a scheme based on image contrast stretching and smoothing operations have been used to allocate the iris outer boundary. Fig. 2 shows samples of detected iris regions using our developed method. The attained localization accuracy rate for this approach was 0.972%. In the next step, only the iris images that successfully localized will be used as test material for evaluating the recognition performance.
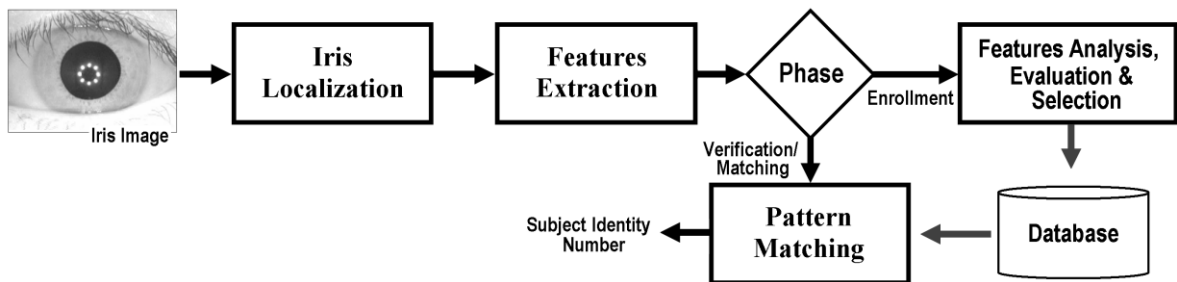

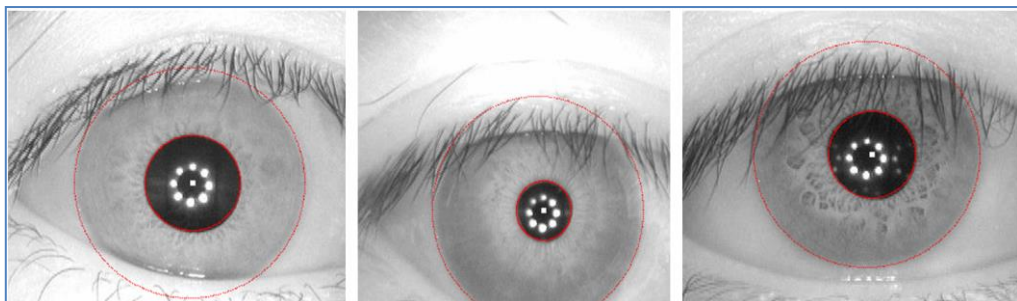Figure 1. The processing stages of the generic iris recognition system model

Figure 2. Samples of successful iris localization for CASIA V4.0 using our developed method

Step-2: (Iris Normalization)

2

The size of the iris varies from person to person, and even for the same person, due to variation in illumination, pupil size and distance of the eye from the camera. These factors can severely affect iris matching performance. In order to get accurate results, it is necessary to eliminate, or even reduce the effect of, these factors. To achieve this, the localized iris area is mapped to be flattened, rectangular area instead of being circular; and to do this mapping task a transformation from polar coordinates (r,θ) to Cartesian coordinates (x,y) is applied upon each point within the iris region. As shown in Fig. 3, the mapping process is accomplished using the following equations:

$$I\left(x_p, y_p\right) \quad \rightarrow \quad I(r,\theta) \quad \rightarrow \quad I(x_f, y_f) \tag{1}$$

Such that,

$$x_f = \frac{W\theta}{2\pi} \quad , \quad y_f = \frac{H(r - R_1)}{R_2 - R_1} \tag{2}$$

Where, the polar coordinates (r,θ) are determined using the pixel's coordinates in the original iris image:

$$\Delta x = x_p - x_c; \qquad \Delta y = y_p - y_c$$

$$\theta = -\tan^{-1}(\frac{\Delta y}{\Delta x}); \qquad r = \sqrt{(\Delta x)^2 + (\Delta y)^2} \tag{3}$$

Where $I(x_p, y_p)$, (x_f, y_f), (r, θ), (x_c, y_c) represent the original iris region, the flattening coordinates, polar coordinates, and the coordinates of the pupil center point. The width (W) and height values of the flattened iris image are taken 720 & 60 respectively.

Step-3: (Proposed Eyelash and Eyelid Removing Method)

One of the many challenging tasks that may need to be handled in iris segmentation is the detection eyelash and eyelid areas in the iris region. As we know eyelid pixel values appear as bright pixels while eyelashes appear as dark pixels. Also, the eyelid appears at the upper side of the iris image while eyelashes may extend from both upper and lower side of the image. In this paper a simple method is proposed to detect the eyelid/ eyelashes pixels, it depends on computing of image the first order image statistical parameters (i.e., the mean and standard deviation).

Step-3-1: Eyelid Detection

A simple method was proposed which depend on computing of image statistic such as mean and standard deviation for eyelid point's detection. To detect these points the mean and standard deviation values of window size (5x5) are calculated where the normalized image has the size (60x720). Then, compare these values for each window with threshold. Binary image *Bimg( )* will created where eyelid point will set to zero and iris point will set to 255. If the mean larger than threshold T_1 and standard deviation value larger than threshold T_2 the center point will be considered as iris point and its value set to 255 in *Bimg( )* otherwise eyelid point and its value set to zero. Fig. 4 show samples result of this step.

(a)

(b)

3

(a)

(b)
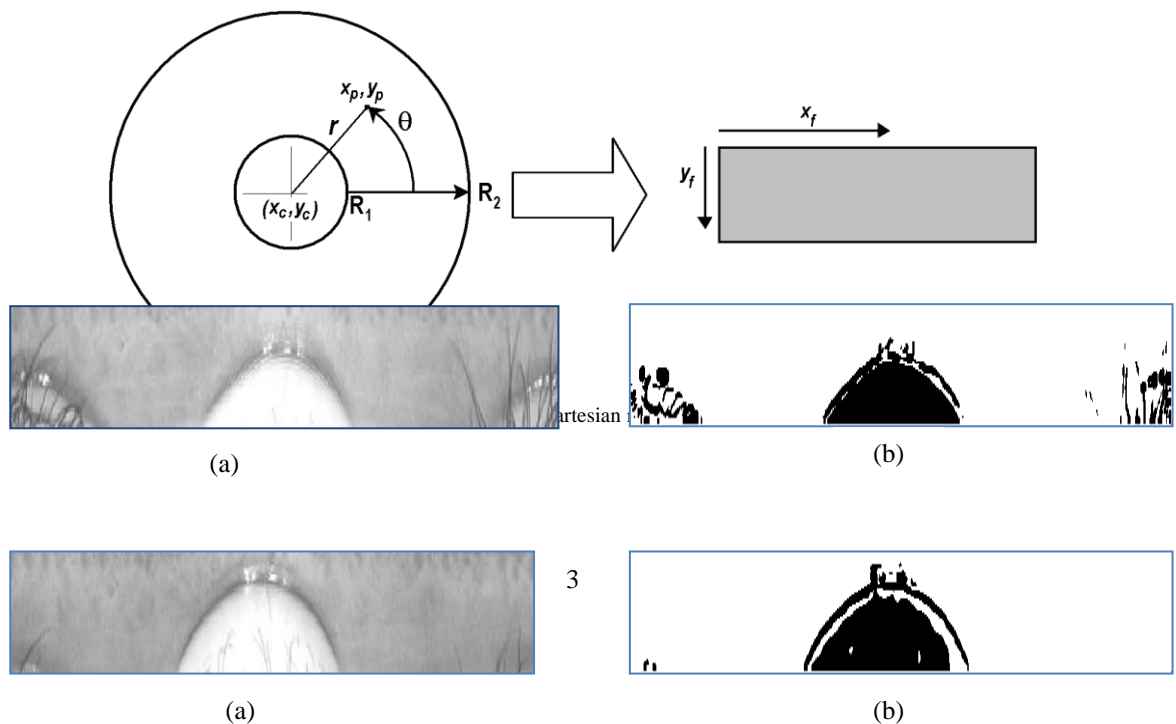
Step-3-2: Eyelash Detection

For eyelash detection a combination of enhancement and soble edge detection processes are used. At first step the enhancement steps will applied to produce $E(\ )$ array. The enhancement process will decrease eyelash point's brightness (i.e. eyelash points become darker). The following steps depicted enhancement process:

Step3-2-1: Compute the mean (m) and standard deviation (σ) of the eye image.
Step3-2-2: Determine the Low and High values according to the following equations:

$$Low = m - \alpha x\sigma, \ High = m + \alpha x\sigma \tag{4}$$

Where, α is the scaling factor whose value is within the range [1, 3].

Step3-2-3: Then, contrast stretching is done by applying the following mapping equation:

$$E(x,y)=\begin{cases} 0 & if \ I(x,y) \leq Low \\ 255\left(\dfrac{I(x,y)-Low}{High-Low}\right) & if \ Low < I(x,y) < High \\ 255 & if \ I(x,y) \geq High \end{cases} \tag{5}$$

Where, $E(x, y)$ is the enhanced image, $I(x, y)$ is the original image.

At second step, soble edge detection will be applied to produce $simg(\ )$. The vertical and horizontal soble masks are given in Fig. 5:

-1	-2	-1
0	0	0
1	2	1

(a)

-1	0	1
-2	0	2
-1	0	1

(a)   (b)

Figure 5. Soble masks (a) horizontal mask   (b) vertical mask

To find the value of edge points the following equation will be use

$$simg(y,x) = \sqrt{S_1^2 + S_2^2} \tag{6}$$

where S_1^2 is edge detection from convolution along vertical mask.
S_2^2 is edge detection from convolution along vertical mask.

Fig. 6 show the result of enhancement and soble edge detection process. The eyelash point will be detected from *simg( )* and *E( )* using thresholding, where two threshold values *T1, T2* are selected based on testing. Each point in *simg( )* array generated from soble edged detector will compare with *T1*, and each point in *E( )* array generated from enhancement process will compare with *T2*. Then the following condition should satisfied

    Check if (simg(x, y)>T1) and (E(x, y)<T2)
      Bimg(x,y)←0
      Elseif
      Bimg(x,y)←255

In order to complete the noisy point's detection, the binary iris image *Bimg( )* will be divided into three regions (R1, R2, and R3). The size of R1 is (60×180), R2 is (60×360) and R3 is (60×180) as shown from Fig. 7. Then each point has the value 255 in *Bimg ( )* array will check its neighbors if at least two points have the value zero will be converted to 255. Fig. 8 shows samples of final detected noisy eyelash and eyelids points in iris images using proposed method.
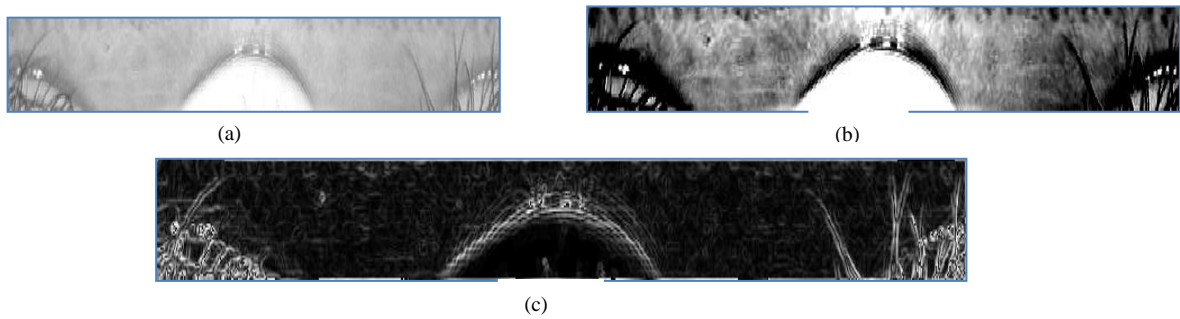

(a)

(b)

(c)

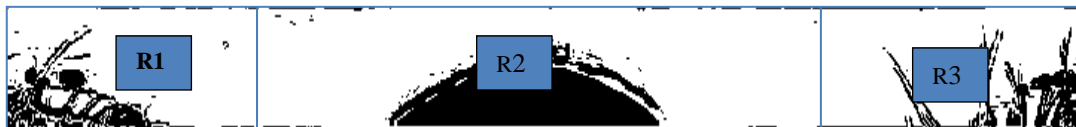Figure 6. Eyelash detection process (a) Original image (b) Enhancement image   (c) Soble image
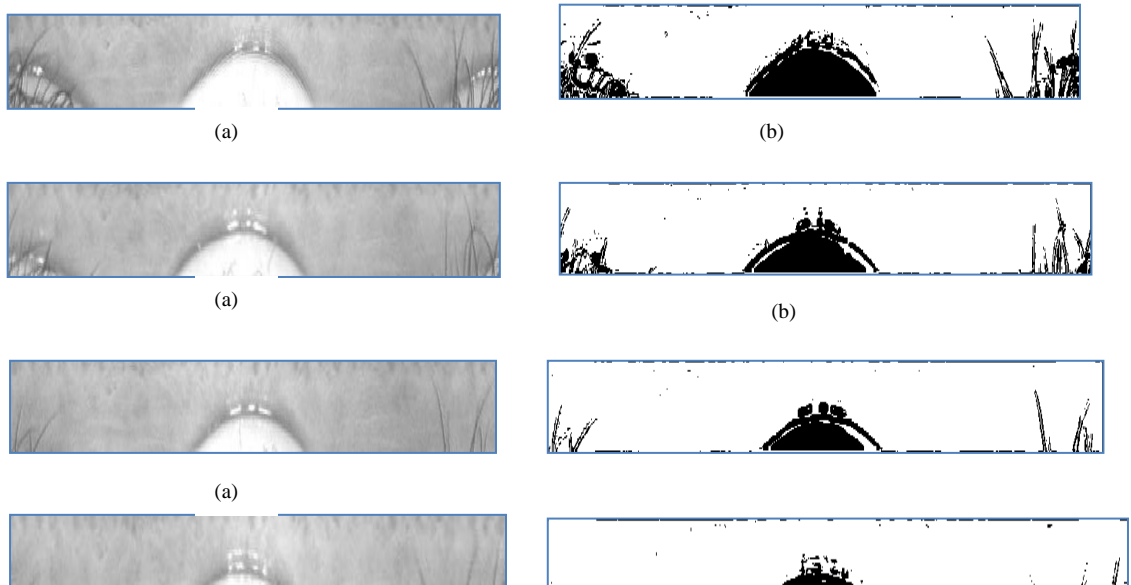

R1

R2

R3

Fig.ure 7. Iris regions R1, R2, R3

(a)

(b)

(a)

(b)

(a)

(b)

(b)

B. *Iris Enhancement*

The iris images may be captured at different illumination conditions (e.g., the variation in light source position may cause different brightness distribution) which in turn may cause problem at recognition stage. To countermeasure such problem the following steps have been applied:

1. Brightness (Background) Image formation: to estimate the background image (i.e., very low frequency component) the mean of each 32x32 block are computed. Then, the cubic spline interpolation had been utilized to reconstruct the spline surface, which in turn is used as an approximation for brightness variation (i.e., the background image).

2. Image Enhancement: Here, the constructed spline image is subtracted from the original iris image, and then the local histogram equalization method is applied upon each 32x32 block of the iris region using the following steps:

a. Create the histogram for the image.

b. Calculate the cumulative distribution function histogram according to the following equation:

$$cdf(g) = \sum_{j=0}^{g} h(j) \quad\quad (6)$$

Where g is a gray value and $h()$ is the image histogram.

c . Calculate the new pixels values by applying the general histogram equalization formula:

$$eh(i) = round\left(\frac{cdf(i) - cdf_{min}}{W_{image} \times H_{image}} \ (L-1) \right) \quad\quad (7)$$

Where cdf_{min} is the minimum value of the cumulative distribution function, $W_{image}xH_{image}$ are the image's number of columns and rows, and L is the number of gray levels.

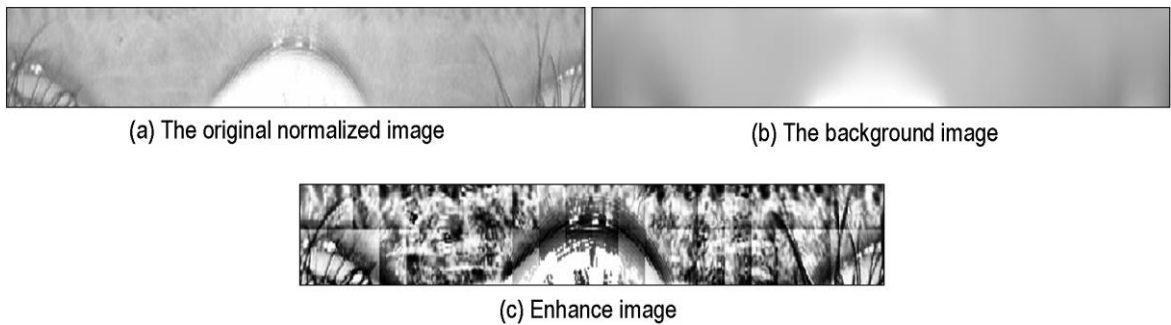Fig. 9 shows a sample of the result produced by our proposed method.

(a) The original normalized image

(b) The background image

(c) Enhance image

Figure 9. Enhancement process

C. Features Extraction

In this phase a set of discriminating iris features is extracted. The adopted set of features consists of texture based features. The features' set is derived from Haar wavelet Matrix. This feature set is calculated by applying the following steps:

1. **Blocks Overlaps:** at first, the normalized image is divided into overlapped blocks with certain overlapping ratio along the vertical and horizontal directions. The block dimensions (W_{block} & H_{block}) in both directions should pre-defined, then the number of blocks (n_x & n_y) along the horizontal and vertical directions, respectively, can be determined by applying the following:

$$n_x = W_{image} \quad div \quad W_{block}$$

$$n_y = H_{image} \quad div \quad H_{block} \tag{8}$$

$$Total \ number \ of \ blocks = n_x \ x \ n_y \tag{9}$$

The blocks' dimensions (W_{block} & H_{block}) and overlapping ratio (r) values have been tested to find the suitable values which lead to best recognition rate. Then for each block do the following steps.

2. **Block Weighting:** to determine the importance of each block, at first the blocks are classified into two classes: *noisy blocks and iris blocks sets.* This classification is done by applying the following criterion:

> ***If number of pixels of the tested block flagged as eyelash or eyelid<(0.95*block size) then***
> > ***The tested Block belong to iris blocks set***
> ***Else***
> > ***Block belong to noisy blocks set***

Noisy blocks will be neglected by assigning the value zero to its weight while other iris blocks are assigned weight value (w) according to the following formula:

$$w(\alpha) = 1 - \frac{1 - \exp(-\mu\alpha)}{1 + \exp(-\mu\alpha)} \tag{10}$$

Where α is parameter its value computed from the following formula:

$$\alpha \ = \ \frac{Number \quad of \quad noisy \quad pixels \quad in \quad the \quad block}{block \quad size} \tag{11}$$

The suitable value of μ parameter is assessed by testing. The value of block weight, w, should be in the range [0, 1]. The conducted tests indicated the blocks lie nearest pupil region take high weight values because they less effect by eyelid and eyelash points, while block weight is more probably decreases at the upper and lower areas which (i.e., near to eyelids and eyelash regions). Fig. 10 presents three iris blocks taken from different iris regions, table I. shows the weight for these blocks (when μ=1).
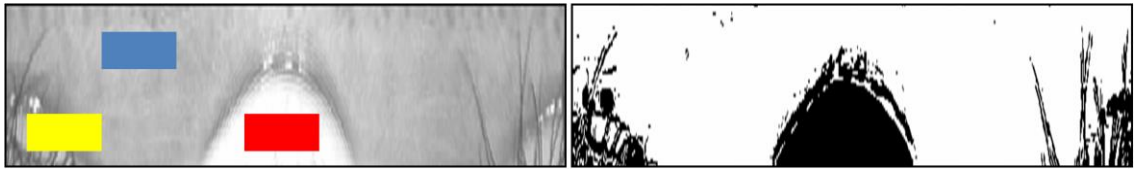

Figure 10. Iris blocks from different iris regions

Table I. Iris blocks from different iris areas with its weight

iris blocks	Block weights	Description
	1	Pure Block: contains only iris points
	0.6	Partial Pure: contains noisy and iris points

	0	Noisy Block: contains only noisy points lie on eyelid region

3. **Features Extraction:** Wavelet transform provides a multi-resolution signal decomposition approach. It decomposes a signal depending on a family of basis functions obtained through translation and dilation of a mother wavelet. In this approach, the advantage of variable window size is taken as a benefit. The window size can be kept wide for low frequencies and narrow for high frequencies which lead to an optimum time-frequency resolution for complete frequency range. When DWT is applied on image, it decomposes the image signal into four sub-bands: approximation (LL) sub-band, and details (LH, HL, HH) subbands [21].

Haar wavelets are the first mother wavelet proposed by Alfred Haar. To calculate Haar subbands the image will be divided into 2x2 block, as shown in Fig. 11, then each value of the four subbands can be calculated using the following (12):

I(2x,2y)	**I(2x+1,2y)**
I(2x,2y+1)	**I(2x+1,2y+1)**

Figure 11. A 2x2 block

$$LL(x, y) = \left(I(x, y) + I(2x+1,2y) + I(2x,2y+1) + I(2x+1,2y+1)\right)/2$$

$$LH(x, y) = \left(I(x, y) - I(2x+1,2y) + I(2x,2y+1) - I(2x+1,2y+1)\right)/2$$

$$HL(x, y) = \left(I(x, y) + I(2x+1,2y) - I(2x,2y+1) - I(2x+1,2y+1)\right)/2$$

$$HL(x, y) = \left(I(x, y) - I(2x+1,2y) - I(2x,2y+1) + I(2x+1,2y+1)\right)/2$$

(12)

Where, $x \in \{0, 1, ..., W_{block}/2-1)\}$ and $y \in \{0, 1, ..., H_{block}/2-1)$

Based on the available wavelet coefficients, the average of absolute coefficients values ($\bar{S}$) and the standard deviation (σ_S) features for each sub-band are calculated from the following formulas:

$$\bar{S} = \frac{1}{W_{block} \, H_{block}} \sum_y \sum_x \left|S(x, y)\right|$$

(13)

$$\sigma_S^2 = \frac{1}{W_{block} \, H_{block}} \sum_y \sum_x \left(S(x, y) - \bar{s}\right)^2$$

(14)

Where, S() represents a wavelet sub-band coefficient (either LL, LH, HL or HH) and $\bar{S}$ is the average value for the sub-band coefficients.

4. **Generation of Iris Feature Vector**: In this step, the Haar wavelet is applied on each iris block separately, then the features list of values $F = \{\bar{S}, \sigma_S\}$ derived from the four subbands are collected and assembled in the feature vector. Then, for each class (person) the iris template, T, is created from the feature vectors belong to different image samples belong to that class. Beside to template vector (T) the degree of variability of each collected feature is represented by computing the standard deviation vector (Ω_T); where each element of this vector represents the degree of scattering of the corresponding feature within a class. To compute the template vectors, the mean and standard deviation values for each feature from different blocks belong to different image sample are determined. The mean and standard deviation vectors are determined using the following equations:

$$t_{ip} = \frac{1}{n_p} \sum_{j=1}^{n_p} f_{ijp} \quad , \quad \omega_{ip} = \sqrt{\frac{1}{n_p} \sum_{j=1}^{n_p} \left(f_{ijp} - t_{ip}\right)^2}$$

(15)

Where, f_{ijp} is the value of the ith feature extracted from j^{th} sample image belong to person p, n_p is the number of images samples taken for p person, t_{ip} is the mean value of the ith feature for person (p), ω_{ip} is the standard deviation of the ith

feature for *p* person. The collection of {t_{ip}| i=1 to m} represent the template vector, *T(p)*, for person (*p*), and the collection of {ω_{ip}| i=1 to m} represent the standard deviation vector, Ω_T (p), for person p.

It is noticed some features, f_{ijp}, have high deflection values relative to their averages. To handle this problem the values of the features which are relatively far from the mean value have been excluded in order to enhance the computation of the template vector. The applied exclusion criterion is:

If |f_{ijp} - t_{ip}| > 2.3ω_{ip} then exclude f_{ijp} & recalculate t_{ip} and ω_{ip}

As a last step, the lowest possible combinations of the features can lead to good recognition is searched for. The test of finding best feature combinations were started using single feature and gradually increased to double, third and so on till reaching the highest recognition rate.

D. *Pattern Matching*

in this step the extracted feature vector of iris image will compare with all templates vectors stored in the database. The Normalized Euclidian (D_E) distance is used as a feature vector similarity measure; the template vector that give minimum value will represent the class of enrolled image:

$$D_E(F_u, j) = \sum_{i=1}^{k} \left| \frac{f_{iu} - t_{ij}}{\omega_{ij}} \right| \tag{16}$$

Where, $F_u = \{f_{1u}, f_{2u}, ..., f_{ku}\}$ is the feature vector of unknown iris image, $T_j = \{t_{1j}, t_{2j}, ..., t_{kj}\}$ is the template vector of person (j), k is the number of used features in the matching stage.

III. EXPERIMENTAL RESULTS

In this section, the attained recognition rates using the introduced method are presented. We thus perform a series of experiments to evaluate its performance. The iris recognition method was tested on the image samples archived in CASIA V1.0 and CASIA V4.0 databases [22], where each iris image has resolution 320×280 pixels. The accuracy of recognition rate (R) was evaluated using the following formula:

$$R = \frac{Number \quad of \quad Correct \quad Identified \quad Iris \quad Images}{Total \quad Number \quad of \quad Iris \quad Images} \times 100\% \tag{17}$$

A. *CASIA V4.0 database*

For each iris class, five image samples have been used for training, while all the images belong to all classes have been used for testing. Most of the published recognition methods were tested on small data sets, in this work the proposed method was tested on 100 classes using, each one has at least six images and above. The subbands of two levels of Haar wavelet have been used as media for feature extraction; such that eight features are computed for each level.

1. Discernment Power of Single features

Fig. 12 presents the attained recognition rates when only one feature is used for representing each iris block. The horizontal axis in the figure represents the index number of the used feature, while the vertical axis represents the attained recognition rate. Fig. 12 shows that the index number of best feature *is fourteen* because it led to highest recognition rate (98.57%), while feature number *nine* led to the lowest recognition rate (89%).

2. Combinations of Two Features

Tests on various combinations of two features have been made. Table II. shows the recognition rates for a small list of best pairs of features. The best attained recognition rate for the pairs two features was (99.6%); which is consist of feature (5) with (14).

3. The Combinations of More Features

Three, four, and ten features have been taken into account to improve the overall success rate of the recognition system. The best recognition rate for combinations of triple features was (99.87%) from combine feature number (5, 7 and 14). While, the best recognition rate for combinations of four features was (100%); which is consist of features (7, 13, 14 and 16).

B. *CASIA V1.0 database*

This database contains 108 persons each of them have seven eye images. all irises were successfully localized. All classes will feed to training stage. Haar wavelet divided each block into four subbands in each level, two levels are used. Then for each subband two features are obtain (i.e. energy and standard deviation). Feature vector will contain sixteen elements. The discernment power of each feature from sixteen features is shown in Fig. 13. Five images are used for

9

training, while all the images belong to all classes have been used for testing. It can show from Fig. 13 that feature index eleven led to best recognition rate. Two, three, four, and five features have been taken into account, the best recognition rate attained for the proposed system for five features is (99.20%); which is consist of features (3, 5, 7, 11 and 14).

Table II The recognition rates for combinations of two features for CASIA V4.0
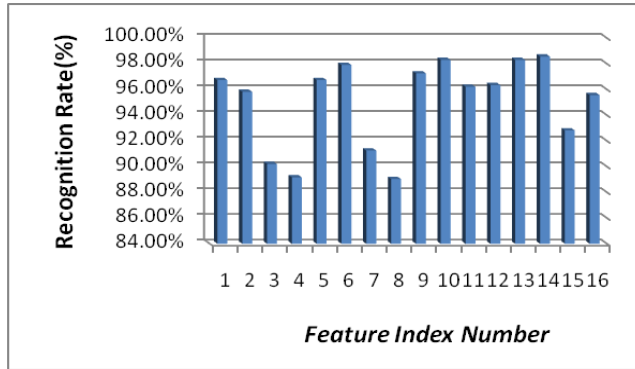

Figure 12. the discrimination power of each feature for CASIA V4.0

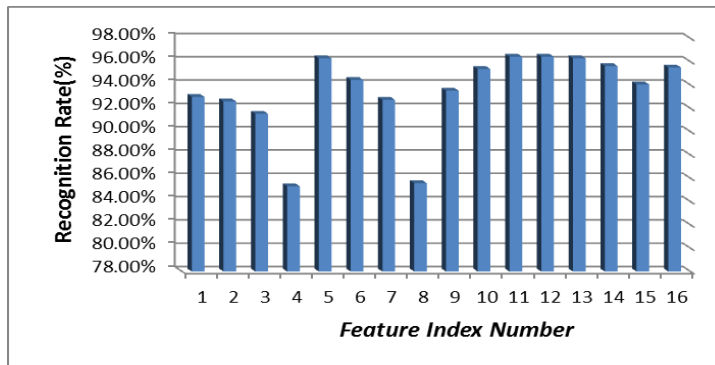| No.	F1 No.	F2 No.	Recognition Rates
1	1	2	98.96%
2	1	6	99.09%
3	1	10	99.09%
4	1	14	99.48%
5	2	5	99.22%
6	2	12	99.22%
7	2	13	99.22%
8	2	15	99.35%
9	2	16	99.22%
10	5	14	99.60%

Figure 13. The discrimination power of each feature for CASIA V1

IV. BEST SELECTION OF SYSTEM PARAMETERS

Several parameters values for the system parameters have been tested and their effects on the recognition rates were investigated. Table III. shows the best registered values for the system parameters that lead to highest recognition rates. To prove the efficiency of our proposed system, the accuracy of our proposed based texture features and some other methods are reported in table IV.

V. CONCLUSIONS

In this paper, a new method was proposed for iris recognition using texture features. Haar wavelet proved to be good iris representation media to provide discriminating features lead to good recognition accuracy. For iris localization we have applied our proposed method that mentioned in [20]. Eyelid and eyelash were detected using image statistics such as the mean and standard deviation, and the test results indicated that this adopted approach gives well results. The mechanism of dividing the iris image into overlapped blocks is suitable because it offers the possibility of reconstructing a feature vector consist of elements each one represent certain area of the iris image. For matching weighted Euclidian distance was used. It is found that:

- The proposed method gives good results and this proves the accuracy of each stage because the efficiency of each stages effect accuracy of recognition rates.
- Detection of eyelids and eyelash from the normalized image, rather than the original iris image, provides simple and fast detection method depending on thresholding.

- The length of best feature vector that representing each iris block consist of four features only; this will reduce the time needed for processing and matching.

Table III. Best selected values for system

Parameter Name	Parameter Value
Overlap ratio	0.1
Block width	20
Block height	20
Image height	60
Image width	720
NX	38
NY	3
Total number of blocks	108

Table IV. The accuracy that achieved by our proposed method based texture and other methods for iris identification

Method	Database Name	Classes Number	Recognition Rate
L.Birgale[17]	CASIA v3	33	99.82%,
Mojtaba [19]	CASIA v1	-	97.96%
K. Gulmire[18]	CASIA v1	10	89.5%.
Our Proposed Method	CASIA v4.	100	100%
Our Proposed Method	CASIA v1	108	99.20%

REFERENCES

[1] Anil K. Jain, Patrick Flynn, Arun A. Ross, "Handbook of Biometrics", Springer, 2007.

[2] Vanaja Roselin, E.Chirchi, Dr. L.M.Waghmare, E.R.Chirchi ,"Enhancement of Person Identification Using Iris Pattern", International Journal of Scientific & Engineering Research, Vol. 2, Issue 4, April-2011.

[3] J. Daugman, "Iris recognition", Am. Scientist 89, pp. 326–333, 2001.

[4] Kevin W. Bowyer, Karen Hollingsworth, Patrick J. Flynn, "Image Understanding for Iris Biometrics: A Survey", Elsevier Computer Vision and Image Understanding, Vol. 110, Pp. 281–307, 2008.

[5] J. Daugman, "High Confidence Visual Recognition of Person by a Test of Statistical Independence", IEEE Transaction on Pattern Analysis and Machine Intelligence, No. 11, Pp. 1148-1161, November- 1993.

[6] J. Daugman, "Statistical Richness of Visual Phase Information: Update on Recognizing Persons by Iris Patterns," International Journal of Computer Vision, Vol. 45, No. 1, Pp. 25–38, 2001.

[7] K.Miyazawa, K. Ito, T. Aoki, K. Kobayashi, and H. Nakajima, "A Phase-Based Iris Recognition Algorithm," in Proceedings of the International Conference on Advances on Biometrics (ICB '06) , Lecture Notes in Computer Science, Vol. 3832, Pp. 356–365, Springer, Hong Kong, January 2006.

[8] C. Sanchez-Avila, R. Sanchez-Reillo, D. de Martin-Roche, "Iris-Based Biometric Recog-nition Using Dyadic Wavelet Transform," IEEE Aerospace and Electronic Systems Magazine ,Vol. 17, No. 10, Pp. 3–6, 2002.

[9] L.Ma, T. Tan, Y. Wang, and D. Zhang, "Efficient iris recognition by characterizing key local variations," IEEE Transactions on Image Processing , vol. 13, no. 6, pp. 739–750, 2004.

[10] R. Sanchez-Reillo and C. Sanchez-Avila, "Iris Recognition with Low Template Size," in Proceedings of the 3rd International Conference on Audio- and Video-Based Biometric Person Authentication (AVBPA '01), Pp. 324–329, Halmstad, Sweden, June 2001.

[11] R. P. Wildes, J. C. Asmuth, G. L. Green, "A Machine Vision System for Iris Recognition," Machine Vision and Applications, Vol. 9, No. 1, Pp. 1–8, 1996.

[12] Y. Zhu, T. Tan, and Y. Wang, "Biometric Personal Identification Based on Iris Patterns," in Proceedings of the 15th International Conference on Pattern Recognition (ICPR '00), Vol. 2, Pp. 801–804, Barcelona, Spain, September 2000.

[13] L. Ma, Y. Wang, and T. Tan, "Iris Recognition Based on Multichannel Gabor Filtering," in Proceedings of the 5th Asian Conference on Computer Vision (ACCV'02), Vol. 1, Pp. 279–283, Melbourne, Australia, January 2002.

[14] K. Bae, S. Noh, and J. Kim, "Iris Feature Extraction Using Independent Component Analysis", in Proceedings of the 4th International Conference on Audio- and Video-Based Biometric Person Authentication (AVBPA'03), Vol. 2688, Pp. 1059–1060, Guildford, UK, June 2003.

[15] Boles, W.W., and Boashash, "A Human Identification Technique Using Images of The Iris and Wavelet Transform", IEEE trans. Signal Processing, Vol.46, No.4, pp.1185-1188, 1998.

[16] Li Ma, T.Tan, "Personal Identification Based on IrisTexture Analysis", IEEE Trans. On Pattern Analysis and Machine Intelligence, Vol.25, No. 12, 2003.

[17] S.J. Sheeba, S.S. Jeya, S. Veluchamy, "Security System Based on Iris Recognition", Research Journal of Engineering Sciences, Vol. 2, No. 3, Pp. 16-21, March 2013.

[18] L.Birgale, M. Korkare, "Iris Recognition Using Ridgelets", journal of Information Processing System, Vol.8, No.3, September 2012.

[19] K. Gulmire, S. Ganorkar, " Iris Recognition Using Independent Component Analysis", International journal of emerging technology and advance engineering, Vol. 2, Issue 7, PP.433-437, July 2012.

[20] Suhad A. Ali, Dr. Loay E. George, "New Method for Iris Localization for Personal Identification", International Conference on Information Technology in Signal and Image Processing-itSIP, India, 2013.

[21] S.S. Kanwaljot, S.K. Baljeet, V.S. Ishpree, "Medical Image Denosing in the Wavelet Domain Using Haar and DB3 Filtering", IRJES Journal, Vol.1, Issue 1, Pp. 1-8, 2012.

[22] Center for Biometrics and Security Research, CASIA Iris Image Database, http://www.cbsr.ia.ac.cn/irisdatabase.